Available online at www.sciencedirect.com

SCIENCE DIRECT®

Journal of Sound and Vibration 273 (2004) 277–294

JOURNAL OF SOUND AND VIBRATION

www.elsevier.com/locate/jsvi

An analytical solution for vibrations of a polarly orthotropic Mindlin sectorial plate with simply supported radial edges

C.S. Huang*, K.H. Ho

Department of Civil Engineering, National Chiao Tung University, 1001 Ta-Hsueh Rd., Hsinchu 30050, Taiwan, ROC

Received 30 September 2002; accepted 28 April 2003

Abstract

This paper presents the first known analytical solution for vibrations of a polarly orthotropic Mindlin sectorial plate with simply supported radial edges. The solution is a series solution constructed using the Frobenius method and exactly satisfies not only the boundary conditions along the radial and circular edges, but also the regularity conditions at the vertex of the radial edges. The moment and shear force singularities at the vertex are exactly considered in the solution. The correctness of the proposed solution is confirmed by comparing non-dimensional frequencies of isotropic plates obtained from the present solution with published data obtained from a closed-form solution. This paper also investigates the effects of elastic and shear moduli on the vibration frequencies of the sectorial plates with free or fix boundary conditions along the circumferential edge. A study is also carried out about the influence of elastic and shear moduli on the moment and shear force singularities at the plate origin ($r = 0$) for different vertex angles.

1. Introduction

There are hundreds of published papers on the free vibrations of complete circular and annular, thin and thick plates [1–5]. However, relatively little research work has been done on sectorial plates even though solutions for sectorial plates with simply supported radial edges can be recovered from solutions for complete circular plates for some special values of vertex angles less than 180°. Based on the classical plate theory for isotropic plates, Ben-Amoz [6], Westmann [7], and Bhattacharya and Bhowmic [8] provided some approximate numerical results for cases with clamped radial edges, while Huang et al. [9] presented an exact solution for cases with simply supported radial edges and various conditions along the circular edge. Experimental results were reported by Maruyama and Ichinomiya [10] for completely clamped sectorial plates. To study the vibrations of polar-orthotropic sector

*Corresponding author. Tel.: +886-3-5712121 x54962; fax: +886-3-5716257.
E-mail address: cshuang@cc.nctu.edu.tw (C.S. Huang).

0022-460X/03/$ - see front matter
doi:10.1016/S0022-460X(03)00501-7

plates, Irie et al. [11] used the Ritz method, while Rubin [12] applied the Frobenius method to develop a series solution for cases with simply supported radial edges.

Based on the Mindlin plate theory, only two articles [13,14] have considered the vibrations of sector plates even though some work has been published on annular sector plates (i.e., Refs. [15–19]). The vibration of a sector plate can be treated as a special case of an annular sector plate. However, the singularities for stress resultants at the apex of a sector plate may cause great difficulty in reducing the solution for an annular sector plate to that for a sector plate. Huang et al. [13] developed an exact solution in terms of ordinary and modified Bessel functions for the case with simply supported radial edges. Liu and Liew [14] applied the differential quadrature method to find the natural frequencies of Mindlin sector plates with various types of boundary conditions. In fact, to avoid stress singularities at the vertex, Liu and Liew [14] analyzed annular plates with the ratio of the inner radius to the outer radius equal to 10^{-5} and with the free boundary condition along the inner circumference.

The present work develops an analytical solution for vibrations of a polar-orthotropic Mindlin sector plate having simply supported radial edges. The analytical solution is a series solution and is constructed using the Frobenius method. From the analytical solution, the variation of stress-resultant singularities at the vertex along with the vertex angle and material properties are also investigated. The validity of the analytical solution is confirmed by comparing non-dimensional frequencies for isotropic plates obtained from the proposed solution with published data obtained from a closed-form solution consisting of non-integer order ordinary and modified Bessel functions of the first and second kinds.

2. Basic equations

It is well-known that the equations of motion for the Mindlin plate theory can be expressed in terms of stress resultants in polar co-ordinates (see Fig. 1) as [20]

$$M_{r,r} + \frac{1}{r} M_{r\theta,\theta} + \frac{M_r - M_\theta}{r} - Q_r = \frac{\rho h^3}{12} \ddot{\psi}_r, \tag{1a}$$

$$M_{r\theta,r} + \frac{1}{r} M_{\theta,\theta} + \frac{2M_{r\theta}}{r} - Q_\theta = \frac{\rho h^3}{12} \ddot{\psi}_\theta, \tag{1b}$$

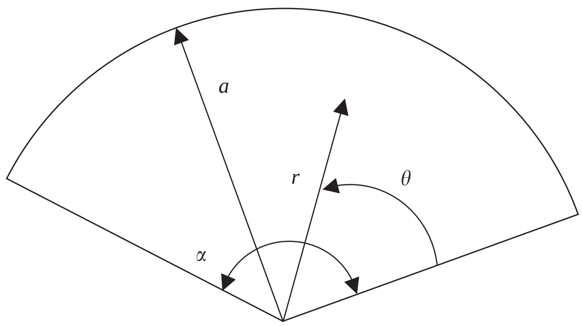

Fig. 1. Defining sketch for a sectorial plate.

$$Q_{r,r} + \frac{Q_r}{r} + \frac{1}{r} Q_{\theta,\theta} = \rho h \ddot{w}, \tag{1c}$$

where ρ is the mass density per unit volume, h is the thickness of the plate, w is the transverse displacement, ψ_r and ψ_θ are the bending rotations of the midplane normal in the radial and circumferential directions, respectively, and "$,\chi$" denotes the differential with respect to the independent variable χ. The differential with respect to time is denoted by a dot. For a polarly orthotropic plate, the stress resultants are related to the transverse displacement and bending rotations by

$$M_r = \frac{h^3}{12}[C_{11}\psi_{r,r} + C_{12}r^{-1}(\psi_r + \psi_{\theta,\theta})], \tag{2a}$$

$$M_\theta = \frac{h^3}{12}[C_{22}r^{-1}(\psi_r + \psi_{\theta,\theta}) + C_{21}\psi_{r,r}], \tag{2b}$$

$$M_{r\theta} = \frac{h^3 G_{r\theta}}{12}[r^{-1}(\psi_{r,\theta} - \psi_\theta) + \psi_{\theta,r}], \tag{2c}$$

$$Q_r = \kappa^2 G_r h(\psi_r + w_{,r}), \tag{2d}$$

$$Q_\theta = \kappa^2 G_\theta h(\psi_\theta + r^{-1}w_{,\theta}), \tag{2e}$$

where

$$C_{11} = \frac{E_r}{1 - \upsilon_{r\theta}\upsilon_{\theta r}},\ C_{12} = \frac{E_\theta \upsilon_{r\theta}}{1 - \upsilon_{r\theta}\upsilon_{\theta r}},\ C_{21} = \frac{E_r \upsilon_{\theta r}}{1 - \upsilon_{r\theta}\upsilon_{\theta r}},\ C_{22} = \frac{E_\theta}{1 - \upsilon_{r\theta}\upsilon_{\theta r}},$$

E_r and E_θ are elastic moduli in the radial and tangential directions, respectively, G_r, G_θ, and $G_{r\theta}$ are shear moduli in the proper directions, υ_{ij} is the Poisson ratio defined as the strain in the j direction due to the unit strain in the i direction, and $\kappa^2 = \pi^2/12$ is the shear correction factor. Notably, C_{12} must be identical to C_{21}.

For free vibration analysis, assume that

$$(\psi_r, \psi_\theta, w) = (\Psi_r, \Psi_\theta, W)e^{i\omega t}. \tag{3}$$

Substituting Eqs. (2) and (3) into Eqs. (1a)–(1c) with arrangement yields

$$\begin{aligned} &\frac{h^3}{12}\{C_{11}\Psi_{r,rr} + (C_{12} + C_{11} - C_{21})r^{-1}\Psi_{r,r} + G_{r\theta}r^{-2}\Psi_{r,\theta\theta} - C_{22}r^{-2}\Psi_r \\ &\quad - (C_{22} + G_{r\theta})r^{-2}\Psi_{\theta,\theta} + (C_{12} + G_{r\theta})r^{-1}\Psi_{\theta,\theta r})\} - \kappa^2 G_r h(\Psi_r + W_{,r}) + \frac{\omega^2 \rho h^3}{12}\Psi_r = 0, \end{aligned} \tag{4a}$$

$$\begin{aligned} &\frac{h^3}{12}\{G_{r\theta}(\Psi_{\theta,rr} + r^{-1}\Psi_{\theta,r} - r^{-2}\Psi_\theta) + C_{22}r^{-2}\Psi_{\theta,\theta\theta} + (C_{21} + G_{r\theta})r^{-1}\Psi_{r,\theta r} \\ &\quad + (C_{22} + G_{r\theta})\Psi_{r,\theta}\} - \kappa^2 G_\theta h(\Psi_\theta + r^{-1}W_{,\theta}) + \frac{\omega^2 \rho h^3}{12}\Psi_\theta = 0, \end{aligned} \tag{4b}$$

$$\kappa^2 G_r h(W_{,rr} + r^{-1}W_{,r} + \Psi_{r,r} + r^{-1}\Psi_r) + \kappa^2 G_\theta h(r^{-1}\Psi_{\theta,\theta} + r^{-2}W_{,\theta\theta}) + \omega^2 \rho h W = 0. \tag{4c}$$

3. Construction of series solutions

To establish the solution for a sector plate with a vertex angle equal to α and with simply supported radial edges, it is assumed that

$$W(r,\theta) = W_n(r)\sin p_n\theta, \tag{5a}$$

$$\Psi_r(r,\theta) = \Psi_{rn}(r)\sin p_n\theta, \tag{5b}$$

$$\Psi_\theta(r,\theta) = \Psi_{\theta n}(r)\cos p_n\theta, \tag{5c}$$

where $p_n = n\pi/\alpha$ and $n = 1, 2, 3, \ldots$. This results in satisfaction of the simply supported boundary conditions along $\theta = 0$ and α exactly. That is,

$$w(r,0,t) = w(r,\alpha,t) = 0, \tag{6a}$$

$$M_\theta(r,0,t) = M_\theta(r,\alpha,t) = 0, \tag{6b}$$

$$\psi_r(r,0,t) = \psi_r(r,\alpha,t) = 0. \tag{6c}$$

By substituting Eqs. (5a)–(5c) into Eqs. (4a)–(4c) and letting $\bar{r} = r/a$ and $\bar{W}_n = W_n/a$, where a is the radius of plate, one can obtain

$$\begin{aligned}\Psi_{rn,\overline{rr}} &+ \frac{C_{11}-C_{21}+C_{12}}{C_{11}}\bar{r}^{-1}\Psi_{rn,\bar{r}} - \left(\frac{C_{22}+G_{r\theta}p_n^2}{C_{11}}\bar{r}^{-2} + \frac{12a^2\kappa^2G_r}{h^2C_{11}} - \frac{\rho a^2\omega^2}{C_{11}}\right)\Psi_{rn}\\ &- \frac{(C_{12}+G_{r\theta})p_n}{C_{11}}\bar{r}^{-1}\Psi_{\theta n,\bar{r}} + \frac{(C_{22}+G_{r\theta})p_n}{C_{11}}\bar{r}^{-2}\Psi_{\theta n} - \frac{12a^2\kappa^2G_r}{C_{11}}\bar{W}_{n,\bar{r}} = 0,\end{aligned} \tag{7a}$$

$$\begin{aligned}\Psi_{\theta n,\overline{rr}} &+ \bar{r}^{-1}\Psi_{\theta n,\bar{r}} - \left[\left(1+\frac{C_{22}p_n^2}{G_{r\theta}}\right)\bar{r}^{-2} + \frac{12a^2\kappa^2G_\theta}{h^2G_{r\theta}} - \frac{\rho a^2\omega^2}{G_{r\theta}}\right]\Psi_{\theta n}\\ &+ \left(1+\frac{C_{21}}{G_{r\theta}}\right)p_n\bar{r}^{-1}\Psi_{rn,\bar{r}} + \left(1+\frac{C_{22}}{G_{r\theta}}\right)p_n\bar{r}^{-2}\Psi_{rn} - \frac{12a^2\kappa^2G_\theta p_n}{h^2G_{r\theta}}\bar{r}^{-1}\bar{W}_n = 0,\end{aligned} \tag{7b}$$

$$\bar{W}_{n,\overline{rr}} + \bar{r}^{-1}\bar{W}_{n,\bar{r}} - \left(\frac{G_\theta p_n^2}{G_r}\bar{r}^{-2} - \frac{\rho a^2\omega^2}{\kappa^2G_r}\right)\bar{W}_n + \Psi_{rn,\bar{r}} + \bar{r}^{-1}\Psi_{rn} - \frac{G_\theta p_n}{G_r}\bar{r}^{-1}\Psi_{\theta n} = 0. \tag{7c}$$

Following the Frobenius method [21] to construct the general series solutions of Eqs. (7a)–(7c), we let

$$\Psi_{rn} = \sum_{m=0,1} a_m\bar{r}^{\,s+m}, \quad \Psi_{\theta n} = \sum_{m=0,1} b_m\bar{r}^{\,s+m} \quad \text{and} \quad \bar{W}_n = \sum_{m=0,1} c_m\bar{r}^{\,s+m+1}, \tag{8}$$

where the characteristic value, s, can be a complex number. The real part of s has to be positive (i.e., $\mathrm{Re}(s)\geqslant 0$) to meet the requirement of regularity conditions at the vertex of a sector domain, namely, finite values for ψ_r, ψ_θ, and w as $\bar{r}$ approaches zero. From the relations between stress resultants and displacement components given in Eqs. (2a)–(2e), it is discovered that the moments are unbounded at the vertex as the real part of s is less than one. Substituting Eq. (8) into

Eqs. (7a)–(7c) with careful arrangement yields

$$\sum_{m=0,1}[((m+s)(m+s-1)+\xi_1(s+m)-\xi_2)a_m+(-\xi_3(s+m)+\xi_4)b_m]\bar{r}^{\,s+m-2}$$
$$+\sum_{m=0,1}\left\{\left(-\xi_5+\frac{\rho a^2\omega^2}{C_{11}}\right)a_m-\xi_5(s+m+1)c_m\right\}\bar{r}^{\,s+m}=0, \quad (9a)$$

$$\sum_{m=0,1}\Bigg\{[(\beta_2(s+m)+\beta_3)a_m+((s+m)^2-\beta_1)b_m]\bar{r}^{\,s+m-2}$$
$$+\left[\left(-\beta_4+\frac{\rho a^2\omega^2}{G_{r\theta}}\right)b_m+\beta_4 p_n c_m\right]\bar{r}^{\,s+m}\Bigg\}=0, \quad (9b)$$

$$\sum_{m=0,1}\left\{\left[\left((s+m+1)^2-\frac{G_\theta p_n^2}{G_r}\right)c_m+(s+m+1)a_m-\frac{G_\theta p_n}{G_r}b_m\right]\bar{r}^{\,s+m-1}+\frac{\rho a^2\omega^2}{\kappa^2 G_r}c_m\bar{r}^{\,s+m+1}\right\}=0, \quad (9c)$$

where

$$\xi_1=(C_{11}-C_{21}+C_{12})/C_{11},\quad \xi_2=(C_{22}+G_{r\theta}p_n^2)/C_{11},\quad \xi_3=(C_{12}+G_{r\theta})p_n/C_{11},$$
$$\xi_4=(C_{22}+G_{r\theta})p_n/C_{11},\quad \xi_5=12a^2\kappa^2G_r/h^2C_{11},\quad \beta_1=1+C_{22}p_n^2/G_{r\theta},$$
$$\beta_2=(1+C_{21}/G_{r\theta})p_n,\quad \beta_3=(1+C_{22}/G_{r\theta})p_n,\quad \text{and}\quad \beta_4=12a^2\kappa^2G_\theta/h^2G_{r\theta}.$$

Satisfying Eqs. (9a)–(9c) results in the vanishing coefficients of $\bar{r}$ with different powers. Consequently, one obtains the following recurrence formulas:

$$((s+m+2)(s+m+1)+\xi_1(s+m+2)-\xi_2)a_{m+2}+(-\xi_3(s+m+2)+\xi_4)b_{m+2}$$
$$=-\left[\left(-\xi_5+\frac{\rho a^2\omega^2}{C_{11}}\right)a_m-\xi_5(s+m+1)c_m\right], \quad (10a)$$

$$(\beta_2(s+m+2)+\beta_3)a_{m+2}+((s+m+2)^2-\beta_1)b_{m+2}$$
$$=-\left[\left(-\beta_4+\frac{\rho a^2\omega^2}{G_{r\theta}}\right)b_m+\beta_4p_nc_m\right], \quad (10b)$$

$$\left((s+m+3)^2-\frac{G_\theta p_n^2}{G_r}\right)c_{m+2}+(s+m+3)a_{m+2}-\frac{G_\theta p_n}{G_r}b_{m+2}=-\frac{\omega^2a^2\rho}{\kappa^2G_r}c_m, \quad (10c)$$

for $m=0,1,2,\ldots$, and

$$[(s+i)(s+i-1)+\xi_1(s+i)-\xi_2]a_i+[-\xi_3(s+i)+\xi_4]b_i=0, \quad (11a)$$

$$[(s+i)\beta_2+\beta_3]a_i+[(s+i)^2-\beta_1]b_i=0, \quad (11b)$$

$$(s+i+1)a_i-\frac{G_\theta p_n}{G_r}b_i+\left[(s+i+1)^2-\frac{G_\theta p_n^2}{G_r}\right]c_i=0, \quad (11c)$$

for $i=0$ or 1.

The values of s are determined by finding a non-trivial solution for a_0, b_0, and c_0, which leads to a $3*3$ determinant of coefficient matrix equal to zero:

$$\begin{vmatrix} \Delta_{11} & \Delta_{12} & 0 \\ \Delta_{21} & \Delta_{22} & 0 \\ \Delta_{31} & \Delta_{32} & \Delta_{33} \end{vmatrix} = 0, \tag{12}$$

where $\Delta_{11} = s(s-1) + \xi_1 s - \xi_2$, $\Delta_{12} = -\xi_3 s + \xi_4$, $\Delta_{21} = \beta_2 s + \beta_3$, $\Delta_{22} = s^2 - \beta_1$, $\Delta_{31} = s+1$, $\Delta_{32} = -G_\theta p_n / G_r$, and $\Delta_{33} = (s+1)^2 - G_\theta p_n^2/G_r$. Apparently, Eq. (12) results in a sixth order polynomial for s. There are six roots for s, and they can be complex roots. Only the roots with positive real parts are used to construct the series solutions in order to meet the requirement of regularity conditions at $r = 0$.

Notably, substituting the obtained values of s into Eqs. (11a)–(11c) with $i = 1$ and Eqs. (10a)–(10c), one will discover that odd values of m in Eq. (8) can be eliminated because they do not produce additional solutions. Hence, odd m will not be considered in the following.

A root with a positive real part will fall into one of the following cases and result in different series solutions:

Case I: The root makes

$$\begin{vmatrix} \Delta_{11} & \Delta_{12} \\ \Delta_{21} & \Delta_{22} \end{vmatrix} = 0$$

but does not cause $\Delta_{33} = 0$. In this case, the relations among a_0, b_0, and c_0 are obtained from Eqs. (11a)–(11c) with $i = 0$. They are

$$b_0 = -(\Delta_{11}/\Delta_{12})a_0 \quad \text{and} \quad c_0 = -\frac{\Delta_{31} - (\Delta_{32}\Delta_{11})/\Delta_{12}}{\Delta_{33}} a_0. \tag{13}$$

The resulting series solution is

$$\begin{Bmatrix} \Psi_{rn} \\ \Psi_{\theta n} \\ \bar{W}_n \end{Bmatrix} = a_0 \sum_{m=0,2} \begin{Bmatrix} \bar{a}_m \\ \bar{b}_m \\ \bar{c}_m \bar{r} \end{Bmatrix} \bar{r}^{\,s+m}, \tag{14}$$

where $\bar{a}_0 = 1$, $\bar{b}_0 = -(\Delta_{11}/\Delta_{12})$, and $\bar{c}_0 = -(\Delta_{31} - (\Delta_{32}\Delta_{11})/\Delta_{12})/\Delta_{33}$. The values of $\bar{a}_m$, $\bar{b}_m$, and $\bar{c}_m$ for $m \geqslant 2$ are determined from Eqs. (10a)–(10c) by replacing a_i, b_i, and c_i for $i = 0, 2, 4, \ldots$ with $\bar{a}_i$, $\bar{b}_i$, and $\bar{c}_i$, respectively.

Case II: The root makes

$$\begin{vmatrix} \Delta_{11} & \Delta_{12} \\ \Delta_{21} & \Delta_{22} \end{vmatrix} = 0 \quad \text{and} \quad \Delta_{33} = 0.$$

In this case, two sub-cases have to be discussed. If the root does not make

$$\begin{vmatrix} \Delta_{21} & \Delta_{22} \\ \Delta_{31} & \Delta_{32} \end{vmatrix} = 0,$$

then Eqs. (11a)–(11c) with $i=0$ result in a trivial solution for a_0, b_0, and c_0, so this root has to be discarded. If the root does make

$$\begin{vmatrix} \Delta_{21} & \Delta_{22} \\ \Delta_{31} & \Delta_{32} \end{vmatrix} = 0,$$

then $b_0 = -(\Delta_{11}/\Delta_{12})a_0$ and a_0 and c_0 are to be determined from boundary conditions. The series solution can be expressed as

$$\begin{Bmatrix} \Psi_{rn} \\ \Psi_{\theta n} \\ \bar{W}_n \end{Bmatrix} = a_0 \sum_{m=0,2} \begin{Bmatrix} \hat{a}_m \\ \hat{b}_m \\ \hat{c}_m \bar{r} \end{Bmatrix} \bar{r}^{s+m} + c_0 \sum_{m=0,2} \begin{Bmatrix} \tilde{a}_m \\ \tilde{b}_m \\ \tilde{c}_m \bar{r} \end{Bmatrix} \bar{r}^{s+m}, \tag{15}$$

where $(\hat{a}_0, \hat{b}_0, \hat{c}_0) = (1, -\Delta_{11}/\Delta_{12}, 0)$ and $(\tilde{a}_0, \tilde{b}_0, \tilde{c}_0) = (0, 0, 1)$. The values of $\hat{a}_m, \hat{b}_m, \hat{c}_m$, $\tilde{a}_m$, $\tilde{b}_m$, and $\tilde{c}_m$ for $m \geqslant 2$ can be determined from Eqs. (10a)–(10c) in a way similar to that used to determine $\bar{a}_m$, $\bar{b}_m$, and $\bar{c}_m$ in Case I.

Case III: The root makes

$$\Delta_{33} = 0 \quad \text{and} \quad \begin{vmatrix} \Delta_{11} & \Delta_{12} \\ \Delta_{21} & \Delta_{22} \end{vmatrix} \neq 0.$$

In this case, $a_0 = b_0 = 0$, which causes the solution form given in Eq. (8) to degenerate to the following expression:

$$\Psi_{rn} = \sum_{m=0} a'_m \bar{r}^{s'+m+1}, \;\; \Psi_{\theta n} = \sum_{m=0} b'_m \bar{r}^{s'+m+1}, \quad \text{and} \quad \bar{W}_n = \sum_{m=0} c'_m \bar{r}^{s'+m}. \tag{16}$$

Again, s' can be complex numbers, and its real part must be positive to satisfy the regularity conditions at $r=0$. The relations of stress resultants and displacement components given in Eqs. (2a)–(2e) reveal that the solution given in Eq. (16) generates unbounded shear forces at $r=0$ when the real part of s' is below one. Substituting Eq. (16) into Eqs. (7a)–(7c) yields the following recursive relations among a'_m, b'_m, and c'_m:

$$\begin{aligned} &((s'+m+3)(s'+m+2) + \xi_1(s'+m+3) - \xi_2)a'_{m+2} + (-\xi_3(s'+m+1) + \xi_4)b'_{m+2} \\ &\quad - \xi_5(s'+m)c'_{m+2} = -\left(-\xi_5 + \frac{\rho a^2 \omega^2}{C_{11}}\right)a'_m, \end{aligned} \tag{17a}$$

$$(\beta_2(s'+m+3) + \beta_3)a'_{m+2} + ((s'+m+3)^2 - \beta_1)b'_{m+2} + \beta_4 p_n c'_{m+2} = \left(\beta_4 - \frac{\rho a^2 \omega^2}{G_{r\theta}}\right)b_m, \tag{17b}$$

$$\left((s'+m+2)^2 - \frac{G_\theta p_n^2}{G_r}\right)c'_{m+2} = -(s'+m)a'_m + \frac{G_\theta p_n}{G_r}b'_m - \frac{\omega^2 a^2 \rho}{\kappa^2 G_r}c'_m \tag{17c}$$

and

$$(s'(s'+1)+\xi_1(s'+1)-\xi_2)a_0'+(-\xi_3(s'+1)+\xi_4)b_0'-\xi_5 s' c_0'=0, \tag{18a}$$

$$((s'+1)\beta_2+\beta_3)a_0'+((s'+1)^2-\beta_1)b_0'+\beta_4 p_n c_0'=0, \tag{18b}$$

$$\left((s')^2-\frac{G_\theta p_n^2}{G_r}\right)c_0'=0. \tag{18c}$$

Again, Eqs. (18a)–(18c) result in a $3*3$ determinant of coefficient matrix equal to zero, namely,

$$\begin{vmatrix} \Delta_{11}' & \Delta_{12}' & \Delta_{13}' \\ \Delta_{21}' & \Delta_{22}' & \Delta_{23}' \\ 0 & 0 & \Delta_{33}' \end{vmatrix}=0, \tag{19}$$

where $\Delta_{11}'=s'(s'+1)+\xi_1(s'+1)-\xi_2$, $\Delta_{12}'=-\xi_3(s'+1)+\xi_4$, $\Delta_{31}'=-\xi_5 s'$, $\Delta_{21}'=\beta_2(s'+1)+\beta_3$, $\Delta_{22}'=(s'+1)^2-\beta_1$, $\Delta_{23}'=\beta_4 p_n$, and $\Delta_{33}'=(s')^2-G_\theta p_n^2/G_r$.

Eq. (19) also gives a sixth order polynomial of s'. The roots with negative real parts are discarded by enforcing the regularity conditions at $r=0$. Similar to a foot for s in Eq. (12), a root for s' falls into one of the following subcases:

Subcase III(a): The root makes

$$\begin{vmatrix} \Delta_{11}' & \Delta_{12}' \\ \Delta_{21}' & \Delta_{22}' \end{vmatrix}=0 \quad \text{and} \quad \Delta_{33}'\neq 0,$$

which causes $c_0'=0$. Hence, the solution form given in Eq. (16) will degenerate into that in Eq. (8). Hence, the root has to be discarded.

Subcase III(b): The root makes

$$\begin{vmatrix} \Delta_{11}' & \Delta_{12}' \\ \Delta_{21}' & \Delta_{22}' \end{vmatrix}=0 \quad \text{and} \quad \Delta_{33}'=0.$$

Similar to Case II, if this root causes

$$\begin{vmatrix} \Delta_{12}' & \Delta_{13}' \\ \Delta_{22}' & \Delta_{23}' \end{vmatrix}\neq 0 \quad \text{and} \quad c_0'=0,$$

then it must also be ejected. If this root generates

$$\begin{vmatrix} \Delta_{12}' & \Delta_{13}' \\ \Delta_{22}' & \Delta_{23}' \end{vmatrix}=0, \quad \text{then } b_0'=-\frac{\Delta_{11}'}{\Delta_{12}'}a_0'-\frac{\Delta_{13}'}{\Delta_{12}'}c_0',$$

and a_0' and c_0' are to be determined from boundary conditions. The resulting series solution is

$$\begin{Bmatrix} \Psi_{rn} \\ \Psi_{\theta n} \\ \bar{W}_n \end{Bmatrix}=a_0'\sum_{m=0,2}\begin{Bmatrix} \hat{a}_m'\bar{r} \\ \hat{b}_m'\bar{r} \\ \hat{c}_m' \end{Bmatrix}\bar{r}^{\,s'+m}+c_0'\sum_{m=0,2}\begin{Bmatrix} \tilde{a}_m'\bar{r} \\ \tilde{b}_m'\bar{r} \\ \tilde{c}_m' \end{Bmatrix}\bar{r}^{\,s'+m}, \tag{20}$$

where $(\hat{a}'_0, \hat{b}'_0, \hat{c}'_0) = (1, -\Delta'_{11}/\Delta'_{12}, 0)$ and $(\tilde{a}'_0, \tilde{b}'_0, \tilde{c}'_0) = (0, -\Delta'_{13}/\Delta'_{12}, 1)$. The values of $\hat{a}'_m, \hat{b}'_m, \hat{c}'_m, \tilde{a}'_m, \tilde{b}'_m$, and $\tilde{c}'_m$ for $m \geqslant 2$ can be determined from the recurrence formulas given in Eqs. (17a)–(17c).

Subcase III(c): The root makes

$$\Delta'_{33} = 0 \quad \text{and} \quad \begin{vmatrix} \Delta'_{11} & \Delta'_{12} \\ \Delta'_{21} & \Delta'_{22} \end{vmatrix} \neq 0.$$

One can determine the relations among a_0, b_0, and c_0 from Eqs. (18a) and (18b), and express the relations as $a'_0 = \bar{a}'_0 c'_0$ and $b'_0 = \bar{b}'_0 c'_0$. Consequently, the series solution is

$$\begin{Bmatrix} \Psi_{rn} \\ \Psi_{\theta n} \\ \bar{W}_n \end{Bmatrix} = c'_0 \sum_{m=0,2} \begin{Bmatrix} \bar{a}'_m \bar{r} \\ \bar{b}'_m \bar{r} \\ \bar{c}'_m \end{Bmatrix} \bar{r}^{\,s'+m}, \tag{21}$$

where the coefficients $\bar{a}'_m, \bar{b}'_m$, and $\bar{c}'_m$ for $m \geqslant 2$ are determined from the recurrence formulas given in Eqs. (17a)–(17c).

Notably, when Eq. (12) or (19) has repeated roots with positive real parts or has real roots differing by an integer, the complete series solutions have to be constructed in a way somewhat different from that given above. The solution corresponding to the smaller root will consist of a series solution multiplied by log $(\bar{r})$ just like the approach usually used to solve a single ordinary differential equation [21]. However, this situation very rarely occurs in the case of an orthotropic plate. It only may happen with very special combinations of the vertex angle and material properties. In the following case studies, this type of solution does not occur, so we will not investigate this solution further. The reader interested in constructing this solution can refer to Ho's thesis [22].

When converting the solutions for a orthotropic plate to those for an isotropic plate, one frequently finds that the real roots of s for Eq. (12) differ by an integer. The real root for s in Case I, say s_1, differs from the real root in Case II, say s_2, by an integer k. That is, $s_1 = s_2 + k$. Special cares are needed to construct the series solution corresponding to s_2. Since there are two undetermined coefficients in Case II solution given in Eq. (15), one cannot add logarithm terms into this solution in the manner just mentioned above. When $s_2 + m$ is less than s_1, the solution is constructed as described in Case II.

When $s_2 + m = s_1$, Eqs. (10a)–(10c) result in a set of linear dependent algebraic equations. Only two of them are linear independent and can be expressed as

$$\begin{bmatrix} \delta_{11} & \delta_{12} & 0 \\ \delta_{21} & \delta_{22} & 0 \end{bmatrix} \begin{Bmatrix} a_m \\ b_m \\ c_m \end{Bmatrix} = \begin{bmatrix} \eta_{11} & \eta_{12} \\ \eta_{21} & \eta_{22} \end{bmatrix} \begin{Bmatrix} a_{m-2} \\ c_{m-2} \end{Bmatrix}, \tag{22}$$

where $\delta_{11} = s_1(s_1 - 1) + \xi_1 s_1 - \xi_2$, $\delta_{12} = -\xi_3 s_1 + \xi_4$, $\delta_{21} = s_1 + 1$, $\delta_{22} = -G_\theta p_n / G_r$, $\eta_{11} = \xi_5 - (\rho\omega^2 a^2)/C_{11}$, $\eta_{12} = \xi_5(s_1 - 1)$, $\eta_{21} = 0$, and $\eta_{22} = -\rho\omega^2 a^2/(\kappa^2 G_r)$. Apparently, c_m in Eq. (22) can be arbitrary number. Assume that c_m equals c_0. The values of a_{m-2} and c_{m-2} can be determined from Eqs. (10a)–(10c) in terms of a_0 and c_0. Then, a_m and b_m can be expressed in terms of a_0 and c_0.

When $s_2 + m > s_1$, the values of a_m, b_m, and c_m can be determined from Eqs. (10a)–(10c), again. Consequently, one obtains the general solution corresponding to s_2 with an expression similar to Eq. (15).

Finally, it should be noted that the general series solutions developed in this section have three undetermined coefficients. These three coefficients are to be determined from three boundary conditions along the circular edge of a sector plate.

4. Convergence studies

The accuracy of the solution developed above depends on the number of terms used in the series solution. To show the validity of the proposed solution, convergence studies were conducted for isotropic and orthotropic sector plates with various vertex angles. The converged results are compared here with those from a closed-form solution for an isotropic plate. Notably, unless otherwise noted, the thickness-to-radius ratio (h/a) and the Poisson ratio $\upsilon_{r\theta}$ are set to be 0.2 and 0.3, respectively, for the numerical results shown in this paper. Only the frequencies corresponding to mode shapes with no radial node lines are considered here.

Table 1 shows the convergence of the non-dimensional frequency parameter, $\omega a^2\sqrt{\rho h/D_r}$, where $D_r = E_r h^3/12(1-\upsilon_{r\theta}^2)$, for isotropic sectorial plates with free boundary conditions along the circumference, namely, $M_r(a,\theta,t) = M_{r\theta}(a,\theta,t) = Q_r(a,\theta,t) = 0$. The mode number ($s$) indicates the order of the frequencies corresponding to mode shapes with no radial node lines. Three

Table 1
Convergence of nondimensional frequency parameters $\omega a^2\sqrt{\rho h/D_r}$ for isotropic sectorial plates with a free circular edge

Vertex angle	Mode no.	Number of terms in the series solution				Huang et al. [13]
	s	15	20	40	60	
60°	1	11.770	11.315	11.314	11.314	11.314
	2	39.396	39.959	39.960	39.960	39.960
	3	70.971	70.863	70.862	70.862	70.863
	4	102.25	102.27	102.27	102.27	102.27
	5	/	132.41	132.87	132.87	132.87
180°	1	/	0.000	0.0000	0.0000	0.0000
	2	/	17.946	17.978	17.978	17.978
	3	/	44.445	44.434	44.434	44.434
	4	/	74.331	74.331	74.331	74.332
	5	/	105.03	105.03	105.03	105.03
330°	1	/	2.1736	2.2498	2.2498	2.2498
	2	19.342	15.313	15.291	15.291	15.291
	3	39.057	40.005	40.008	40.008	40.008
	4	68.809	68.775	68.775	68.775	68.775
	5	98.308	98.984	98.983	98.983	98.983

/ : No corresponding data were found.

Table 2
Convergence of frequency parameters $\omega a^2\sqrt{\rho h/D_r}$ for orthotropic sectorial plates with a free circumference and $\alpha = 330^\circ$

E_r/E_θ	Mode no.	Number of terms in the series solution			
	s	15	20	40	60
1/10	1	/	4.0089	6.6322	6.6322
	2	/	33.905	32.713	32.713
	3	/	68.618	69.259	69.259
	4	132.73	114.94	114.73	114.73
	5	208.91	161.92	165.31	165.31
10	1	/	1.0248	1.0835	1.0835
	2	9.3624	8.0723	8.0527	8.0527
	3	31.206	20.496	20.496	20.496
	4	40.148	31.014	31.014	31.014
	5	42.414	41.568	41.568	41.568

/ : No corresponding data were found.

different vertex angles were considered, namely, $\alpha = 60^\circ$, 180°, and 330°. The solutions for the cases of $\alpha = 60^\circ$ and 180° were established from the solution forms given in Eqs. (14) and (15) with the corresponding roots of Eq. (12) differing by an integer, while the solution for $\alpha = 330^\circ$ was developed from Eqs. (14) and (20). Results listed in Table 1 reveal that 40 terms are needed for each of the series solutions to obtain results with five-significant-figure convergence.

Table 1 also lists the results from an exact analytical solution consisting of non-integer order ordinary and modified Bessel functions of the first and second kinds obtained by Huang et al. [13]. Comparison between the present results and the results given by Huang et al. [13] reveals that the present results converge to the exact solution with slight differences in the fifth significant figure. This verifies the correctness of the proposed solution.

Table 2 summarizes the non-dimensional frequencies for orthotropic sectorial plates having a vertex angle of 330° obtained by using different numbers of terms in the series solutions. Two values of E_r/E_θ, 0.1 and 10, were considered. In both cases, the shear moduli G_r, G_θ, and $G_{r\theta}$ were set to be $0.4E_\theta$. In these cases, free boundary conditions were considered along the circumference. The solutions were established from the solution forms given in Eqs. (14) and (20). Like the data given in Table 1, 40 terms in the series solution are needed to obtain the results with five-significant-figure convergence. The data shown in Tables 1 and 2 indicate that as the number of terms increases, the results may converge to the exact values in an oscillatory manner. Furthermore, the data for smaller E_r/E_θ converge somewhat slowly.

5. Numerical results

Tables 3 and 4 list the accurate non-dimensional frequency parameter, $\omega a^2\sqrt{\rho h/D_r}$, for orthotropic sectorial plates with free boundary conditions along the circumferential edge, while

Table 3
Frequency parameters $\omega a^2\sqrt{\rho h/D_r}$ for orthotropic sectorial plates with a free circular edge and various h/a ($G_r = G_\theta = G_{r\theta} = 0.4E_\theta$ and $E_r = 5E_\theta$)

h/a	s	Vertex angle (α, deg)										
		30	60	90	120	150	180	195	210	270	330	360
—	1	22.387	6.2681	2.8892	1.5515	0.8081	0.0000	0.7050	0.9503	1.3969	1.5828	1.6394
	2	64.155	31.097	22.438	18.598	16.473	15.146	15.336	15.485	15.847	16.026	16.084
	3	128.10	78.122	63.975	57.459	53.775	51.439	51.792	52.068	52.733	53.063	53.168
	4	211.22	144.50	124.87	115.66	110.40	107.05	107.54	107.92	108.85	109.31	109.46
0.1	1	17.920	4.8460	2.1247	1.3582	0.7491	0.0000	0.5532	0.7418	1.2469	1.5027	1.5846
	2	51.722	27.656	20.578	17.303	15.547	14.351	14.052	13.806	13.222	12.901	12.755
	3	87.642	58.705	49.616	45.323	42.635	40.893	40.350	39.887	38.572	37.674	37.322
	4	122.05	90.954	80.938	76.036	73.091	71.095	70.416	69.819	68.031	66.821	66.331
0.2	1	15.862	4.7121	2.0990	1.0706	0.5265	0.0000	0.4945	0.6938	1.1167	1.3164	1.3785
	2	37.634	21.809	16.779	14.344	12.914	11.973	11.648	11.370	10.562	10.020	9.8050
	3	55.916	39.375	33.956	31.283	29.694	28.639	28.254	27.921	26.929	26.254	25.987
	4	71.977	55.150	49.605	46.849	45.197	44.092	43.667	43.299	42.208	41.481	41.200
0.4	1	11.831	4.2279	2.0231	1.0685	0.5375	0.0000	0.4403	0.6050	0.9208	1.0471	1.0808
	2	22.875	14.261	11.322	9.8339	8.9268	8.3098	8.0691	7.8606	7.2419	6.8300	6.6704
	3	30.763	21.639	18.795	17.462	16.703	16.219	16.089	15.971	15.587	15.303	15.188
	4	39.689	30.830	21.792	20.623	20.022	19.666	19.558	19.474	19.277	19.187	19.160

—: From classical plate theory.

Figs. 2 and 3 depict the variation of $\omega a^2\sqrt{\rho h/D_r}$ with vertex angles for orthotropic sectorial plates with fixed boundary conditions along the circumference, namely, $w(a,\theta,t) = \psi_r(a,\theta,t) = \psi_\theta(a,\theta,t) = 0$. Again, only the frequencies corresponding to mode shapes with no radial node lines were considered. The results were obtained by using 60 terms in the series solution. The effects of h/a on the frequencies are shown in Table 3, in which the results shown are for the material properties, $G_r = G_\theta = G_{r\theta} = 0.4E_\theta$ and $E_r = 5E_\theta$. Table 4 and Fig. 2 show the results for $G_r = G_\theta = G_{r\theta} = 0.4E_\theta$ and the effects of E_r/E_θ on the frequencies for various vertex angles. Fig. 3 depicts the effects of the shear moduli on the frequencies obtained by setting $E_r/E_\theta = 5$ and $G_r = G_\theta = G_{r\theta} = \gamma E_\theta$, where γ is given in the legend of Fig. 3. Notably, the numbers in parentheses in the legends of Figs. 2 and 3 denote the modal numbers.

The results given in Table 3 indicate that for a constant vertex angle, the non-dimensional frequency parameter, $\omega a^2\sqrt{\rho h/D_r}$, decreases with the increase of h/a not only because of the inherent shear deformation and rotary inertia, but also because $1/h$ is involved in the definition of the frequency parameter. Notably, as h/a increases, an alternative form of the non-dimensional frequency parameter, $\omega a\sqrt{\rho/E_r}$, increases in the lower modes, while this parameter decreases in some of the higher modes. The latter situation occurs when the thickness-shear modes appear among the frequencies shown.

Comparing the results shown in Table 3 for the Mindlin plate theory with those obtained by using series solutions based on classical plate theory [22] reveals that, as expected, the former are

Table 4
Frequency parameters $\omega a^2\sqrt{\rho h/D_r}$ for orthotropic sectorial plates with a free circumferential edge and various E_r/E_θ ($G_r = G_\theta = G_{r\theta} = 0.4E_\theta$)

E_r/E_θ	s	Vertex angle (α, deg)										
		30	60	90	120	150	180	195	210	270	330	360
1/10	1	120.66	37.081	16.432	8.2034	3.9153	0.0000	1.4157	2.5028	5.2669	6.6322	7.0549
	2	212.80	104.499	69.896	53.686	44.569	38.868	37.271	36.108	33.702	32.713	32.403
	3	271.21	156.93	117.18	97.437	85.854	78.366	76.285	74.715	71.090	69.259	68.612
	4	335.66	212.18	168.88	147.00	133.99	125.49	123.24	121.51	117.20	114.73	113.79
1/3	1	65.481	20.196	9.0097	4.5383	2.1907	0.0000	0.8697	1.4631	2.9706	3.7285	3.9662
	2	123.61	62.187	42.688	33.449	28.164	24.789	23.901	23.249	21.859	21.238	21.028
	3	171.19	103.66	80.420	68.794	61.865	57.292	56.125	55.221	52.965	51.641	51.127
	4	219.67	148.19	122.87	109.95	102.14	96.929	95.641	94.594	91.673	89.722	88.936
3	1	20.986	6.4147	2.9071	1.5036	0.7493	0.0000	0.5266	0.7584	1.2818	1.5397	1.6213
	2	47.411	26.675	20.049	16.847	14.973	13.749	13.369	13.052	12.162	11.586	11.358
	3	70.415	48.439	41.099	37.444	35.259	33.807	33.306	32.875	31.593	30.720	30.373
	4	90.780	68.701	61.229	57.475	55.214	53.701	53.138	52.650	51.192	50.212	49.830
10	1	10.504	2.7729	1.0885	0.4711	0.1785	0.0000	0.4519	0.6186	0.9428	1.0835	1.1252
	2	27.221	16.360	12.949	11.289	10.301	9.6397	9.3851	9.1650	8.5045	8.0527	7.8726
	3	40.327	29.072	25.492	23.755	22.732	22.057	21.804	21.585	20.935	20.496	20.324
	4	51.862	40.185	36.433	34.589	33.488	32.750	32.464	32.218	31.492	31.014	30.830

smaller than the latter, and that their differences increase with the increase of h/a. For the second to fourth modes and $\alpha \geqslant 180^\circ$, the non-dimensional frequencies for the Mindlin plate theory decrease with the increase of α, while the results for classical plate theory show the opposite trend.

Table 4 and Fig. 2 indicate that for a constant vertex angle, the non-dimensional frequency parameter, $\omega a^2\sqrt{\rho h/D_r}$, decreases as E_r/E_θ increases because E_r is involved in the definition of the frequency parameter, while Fig. 3 shows an increase of the non-dimensional frequencies with the increase of the shear moduli. However, it should be noted that for a constant vertex angle, the frequency ω increases with the increase of E_r/E_θ. For constant material properties, the frequencies decrease as α increases because the circumferential distance between the radial supports increases with increasing α so that the stiffness of the plate decreases. However, in the case of free boundary conditions along the circumferential edge, the frequencies of the first mode decrease when α increases up to 180°, and then they increase as α goes further away from 180°. This is because the first mode frequency is equal to zero (a rigid-body mode) when α is 180°.

6. Singularities in stress resultants

From the relations between the displacement components and stress resultants given in Eqs. (2a)–(2e), one finds that the solution given in Eq. (8) results in unbounded moments at $r = 0$

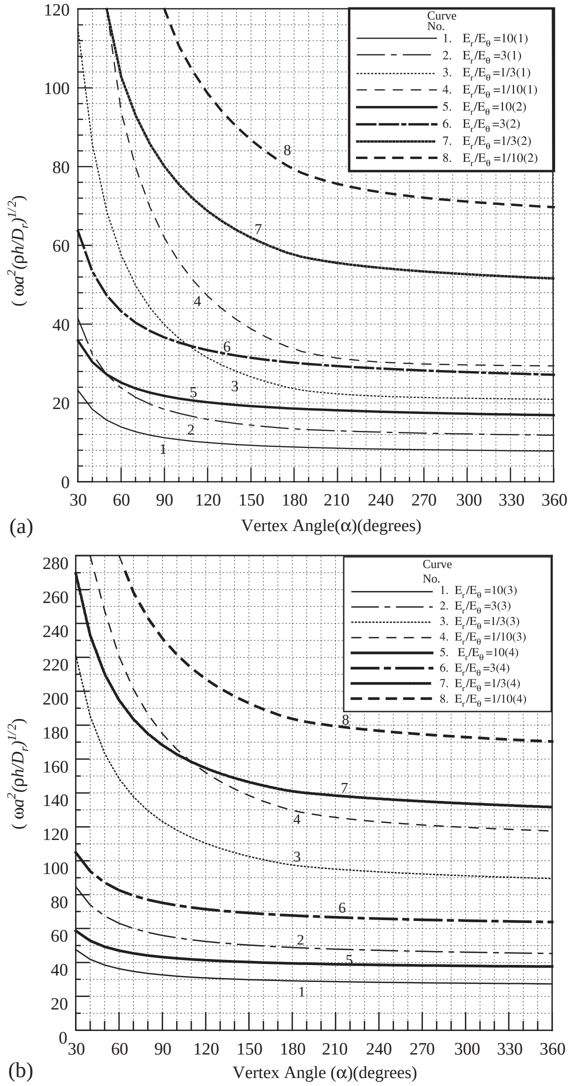

Fig. 2. Variation of $\omega a^2\sqrt{\rho h/D_r}$ with vertex angle for sector plates having a fixed circular edge and various E_r/E_θ (a) for 1st and 2nd modes, (b) for 3rd and 4th modes.

when the real part of s is below one, while the solution given in Eq. (16) produces unbounded shear forces when the real part of s' is less than one. These phenomena will not be affected by the boundary conditions specified along the circular edge of a sectorial plate. Based on the discussion in Section 3, it is found that s is the root of the following fourth order polynomial:

$$s^4 + (p_n^2(\upsilon_{\theta r} - E_\theta/G_{r\theta} + \upsilon_{r\theta}E_\theta/E_r) - E_\theta/E_r - 1)s^2 + E_\theta/E_r(-1 + p_n^2)^2 = 0, \tag{23}$$

and that

$$s' = \sqrt{G_\theta/G_r}p_n. \tag{24}$$

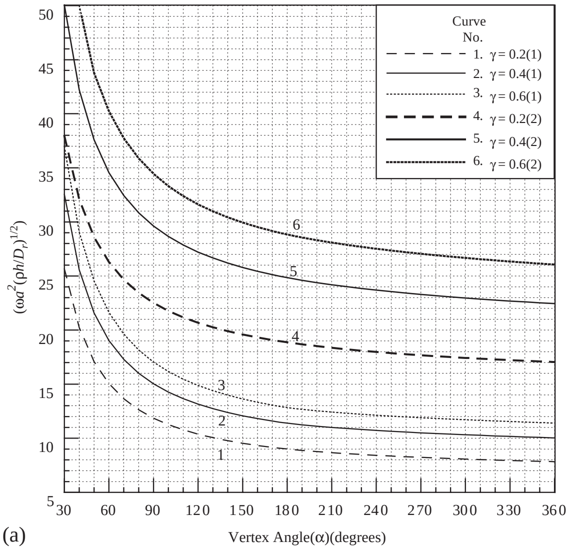

(a)

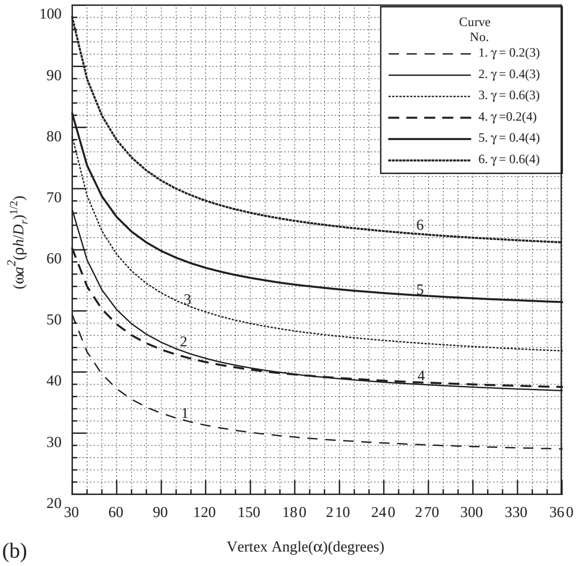

(b)

Fig. 3. Variation of $\omega a^2\sqrt{\rho h/D_r}$ with vertex angle for sector plates having a fixed circular edge and various shear moduli (a) for 1st and 2nd modes, (b) for 3rd and 4th modes.

Eqs. (23) and (24) show that for a constant value of p_n, the moment singularity order is dependent on the elastic moduli, the Poisson ratios, and $G_{r\theta}$ but is not dependent on G_r or G_θ, while the shear force singularity order only depends on G_θ/G_r.

For vibration modes with no radial node lines, shown in Figs. 4a and b are the minimum positive real part of s varying with the vertex angle. The results shown in Figs. 4a and b are for $\upsilon_{r\theta} = 0.3$. We consider different ratios for E_r/E_θ with $G_{r\theta}/E_\theta = 0.4$ in Fig. 4a, and consider different ratios for $G_{r\theta}/E_\theta$ with $E_r/E_\theta = 5$ in Fig. 4b. For a constant vertex angle, larger E_r/E_θ or

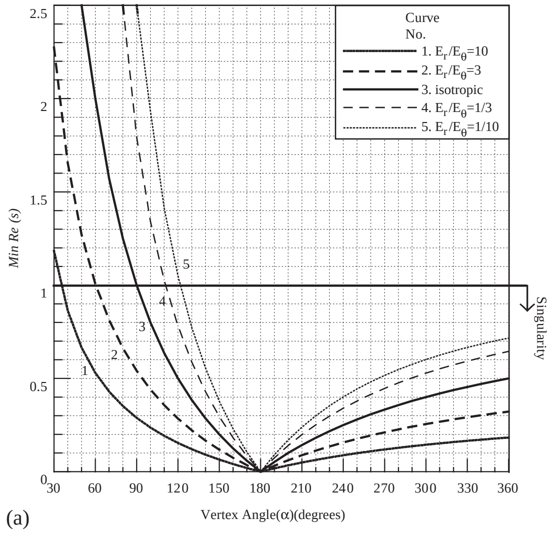

(a)

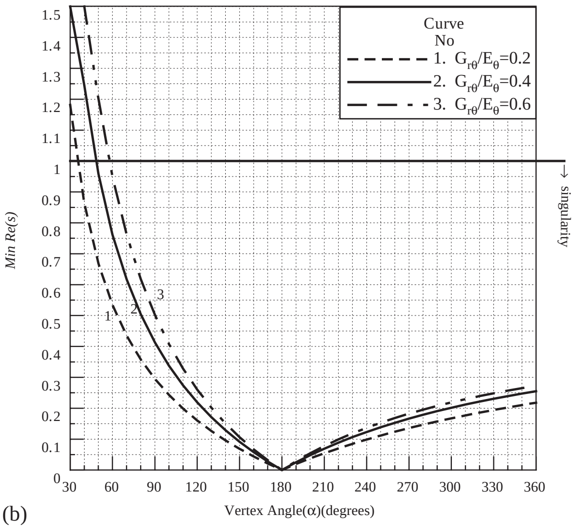

(b)

Fig. 4. Variation of minimum Re(s) with vertex angle (a) for different E_r/E_θ, (b) for different $G_{r\theta}/E_\theta$.

smaller $G_{r\theta}/E_\theta$ produces more severe moment singularities, and smaller G_θ/G_r generates stronger singularities in shear forces. For fixed material properties, the moment singularities in vibration modes with no radial node lines become stronger as α gets closer to 180°, and there is no singularity for $\alpha = 180°$.

Fig. 5 displays the variation of minimum s' with respect to the vertex angle for different values of G_r/G_θ. The results show that the shear singularity becomes more severe as G_r/G_θ or the vertex angle becomes larger. Strangely but interestingly, when G_r/G_θ is larger than one, the singularity occurs even when the vertex angle is equal to 180°. Notably, the results for isotropic material shown in Fig. 5 are identical to those obtained from a closed-form solution by Huang et al. [13].

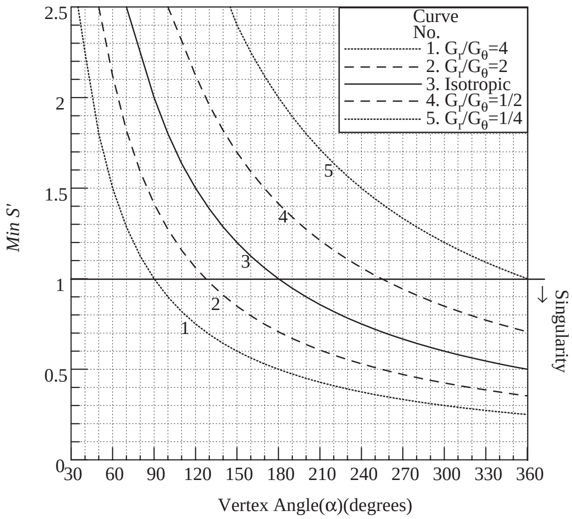

Fig. 5. Variation of minimum s' with vertex angle for various G_r/G_θ.

7. Concluding remarks

It is known that there is no closed-form solution for the vibrations of a polarly orthotropic Mindlin sectorial plate with simply supported radial edges. This paper has presented the first known series solution for such problems obtained by using the Frobenius method. The series solution exactly describes the possible singular behaviors of stress resultants at the vertex of a sectorial plate. The non-dimensional frequencies of an isotropic plate with simply supported radial edges obtained from the present solution have been compared with those obtained from a closed solution and found to be in excellent agreement with the latter.

The proposed solution has been applied to determine the vibration frequencies of sectorial plates with a free or fixed circumferential edge and various elastic moduli. Non-dimensional frequencies corresponding to no radial node line modes have been presented for a wide range of vertex angles ($30^\circ \leqslant \alpha \leqslant 360^\circ$) and $E_r/E_\theta = 0.1$, 1/3, 3, and 10. These unprecedented and accurate results can be used by future investigators to compare with data obtained using alternative analytical methods.

The solution has also been applied to study the effects of elastic and shear moduli on the singular behaviors of moments and shear forces at the vertex. It has been found that the singularity of moments is independent of the shear moduli in the radial and tangential directions (G_r and G_θ), while the singularity of shear forces is only dependent on G_θ/G_r and the value of the vertex angle (α). The singularity of moments becomes stronger as α gets closer to 180°, but there is no singularity for $\alpha = 180^\circ$. The moment singularity also becomes more severe as E_r/E_θ gets larger or $G_{r\theta}/E_\theta$ gets smaller. The singularity of shear forces becomes stronger as G_r/G_θ or α gets larger. When G_r/G_θ is larger than one, there is a shear force singularity, even for the case where $\alpha = 180^\circ$.

Acknowledgements

This work reported herein was supported by the National Science Council, ROC through research Grant No. NSC91-2211-E-009-039. This support is gratefully acknowledged.

References

[1] A.W. Leissa, Vibration of plates, NASA SP-160, US Government Printing Office, 1969.
[2] A.W. Leissa, Recent research in plate vibrations (1973–1976), *Shock and Vibration Digest* 10 (12) (1978) 21–35.
[3] A.W. Leissa, Plate vibration research (1976–1980), *Shock and Vibration Digest* 13 (10) (1981) 19–36.
[4] A.W. Leissa, Recent studies in plate vibrations: 1981–1985, part I: classical theory, *Shock and Vibration Digest* 19 (2) (1987) 11–18.
[5] A.W. Leissa, Recent studies in plate vibrations: 1981–1985, part II: complicating effects, *Shock and Vibration Digest* 19 (3) (1987) 10–24.
[6] M. Ben-Amoz, Note on deflections and flexural vibrations of clamped sectorial plates, *Journal of Applied Mechanics, American Society of Mechanical Engineers* 26 (1) (1959) 136–137.
[7] R.A. Westmann, A note on free vibrations of triangular and sector plates, *Journal of the Aerospace Science* 29 (9) (1962) 1139–1140.
[8] A.P. Bhattacharya, K.N. Bhowmic, Free vibration of a sectorial plate, *Journal of Sound and Vibration* 41 (4) (1975) 503–505.
[9] C.S. Huang, A.W. Leissa, O.G. McGee, Exact analytical solutions for the vibrations of sectorial plates with simply-supported radial edges, *Journal of Applied Mechanics, American Society of Mechanical Engineers* 60 (1993) 478–483.
[10] K. Maruyama, O. Ichinomiya, Experimental investigation of free vibrations of clamped sector plates, *Journal of Sound and Vibration* 74 (4) (1981) 563–573.
[11] T. Irie, G. Yamada, F. Ito, Free vibration of polar-orthotropic sector plates, *Journal of Sound and Vibration* 67 (1) (1979) 89–100.
[12] C. Rubin, Vibrating modes for simply supported polar-orthotropic sector plates, *The Journal of the Acoustical Society of America* 58 (4) (1975) 841–845.
[13] C.S. Huang, O.G. McGee, A.W. Leissa, Exact analytical solutions for free vibrations of thick sectorial plates with simply supported radial edges, *International Journal of Solids and Structures* 31 (11) (1994) 1609–1631.
[14] F.L. Liu, K.M. Liew, Free vibration analysis of Mindlin sector plates: numerical solutions by differential quadrature method, *Computer Methods in Applied Mechanics and Engineering* 177 (1999) 77–92.
[15] P.R. Benson, E. Hinton, A thick finite strip solution for static, free vibration at stability problems, *International Journal for Numerical Methods in Engineering* 10 (1976) 665–678.
[16] P. Guruswamy, T.Y. Yang, A sector element for dynamic analysis of thick plates, *Journal of Sound and Vibration* 62 (4) (1979) 505–516.
[17] R.S. Srinivasan, V. Thiruvenkatachari, Free vibration of transverse isotropic annular sector Mindlin plates, *Journal of Sound and Vibration* 101 (2) (1985) 193–210.
[18] Y. Xiang, K.M. Liew, S. Kitipornchai, Transverse vibration of thick annular sector plates, *Journal of Engineering Mechanics, American Society of Civil Engineers* 119 (8) (1993) 1579–1599.
[19] K.M. Liew, S. Kitipornchai, Y. Xiang, Vibration of annular sector Mindlin plates with internal radial line and circumferential arc supports, *Journal of Sound and Vibration* 183 (3) (1995) 401–419.
[20] R.D. Mindlin, H. Deresiewicz, Thickness-shear and flexural vibrations of a circular disk, *Journal of Applied Physics* 25 (1954) 1329–1332.
[21] F.B. Hildebrand, *Advanced Calculus for Applications*, 2nd Edition, Prentice-Hall, Inc., New York, 1976.
[22] K.H. Ho, Analytical Solution for Sectorial Plates with Simply-supported Radial Edges Based on Various Plate Theories, MS Thesis, National Chiao Tung University, Hsinchu, Taiwan, 2002.